Behavior of a Chiral Liquid Crystalline Polysiloxane at the Air/Water Interface

Xiao Chen, Qing-Bin Xue, and Kong-Zhang Yang*

Institute of Colloid and Interface Chemistry, Shandong University, Jinan 250100, China

Qi-Zhen Zhang

Department of Chemistry, Shandong University, Jinan 250100, China

Received December 7, 1995; Revised Manuscript Received May 9, 1996[⊗]

ABSTRACT: The monolayer behaviors at the air/water interface of a newly synthesized side chain liquid crystalline polymer (PLC-4) and its constituent monomer (MLC-4) have been investigated by means of surface pressure−area isotherms, hysteresis curves, and UV−vis spectroscopy. The orientation and packing of molecules in the monolayer with compression are discussed. The ability to form Langmuir−Blodgett films was investigated.

Introduction

Liquid crystalline polymers (PLC) are of wide interest due to their self-ordering capabilities, with the added advantage over low molecular weight compounds of greater mechanical and thermal stabilities. PLC has already been applied to optical storage,[1] nonlinear optical devices,[2−4] ferroelectric switching,[5] and so forth.[6,7] Thus, scientists are more interested in how to assemble PLC molecules to form monolayers or multilayers with defined thicknesses and structures, which is usually difficult to obtain in smectic liquid crystalline systems.

Using the Langmuir−Blodgett technique, it is convenient to form ordered layer structures by transferring PLC monolayers from the water surface to solid substrates.[8,9] This ordered deposition offers potentially greater control over molecular orientation and intermolecular packing for these materials, which could lead to more and more creations of new types of thin-film devices, especially in the field of electronics and optics.[10,11] Research work on the behavior of PLC monolayers and LB films has attracted increasing attention in recent years.[12−23] Among them, the side chain liquid crystalline polymer appears to be more noticeable. Different functional mesogenic units can be incorporated into the side chains separated from the backbone by flexible spacers, which not only improve the deposition conditions for a rigid and viscous polymer monolayer but also enhance the ultimate ordering in the built-up multilayer film and provide new functions.

When building up LB films of a LC material, it is of great importance to get information about the structure of the underlying monolayer. Not only the orientation normal to the subphase (tilt angle) is of importance but also the nature and uniformity of the positional and tilt order in the film plane (and resulting morphology and domain size).

In our previous paper, we reported the monolayer behavior of a chiral polysiloxane with a Schiff-base mesogenic side chain.[24] However, small changes in the molecular structure of the LC polymer (for example, type of mesogen) have an immense influence on the monolayer properties. On the basis of this consideration, we have chosen another newly synthesized side chain liquid crystalline polymer with a biphenyl mesogenic side chain (denoted as PLC-4) to investigate changes of the monolayer behavior and LB multilayer preparation. The chemical structure of PLC-4 is shown in Figure 1 together with its thermal bulk phase behavior. Also shown in Figure 1 is its monomeric side chain (labeled MLC-4). The monolayer property of MLC-4 has also been studied as a comparison. It would be interesting to characterize and compare the behaviors of these two molecules, as both of them contain a chiral center at the same location and can be induced to the smectic C* phase to exhibit ferroelectricity.[25]

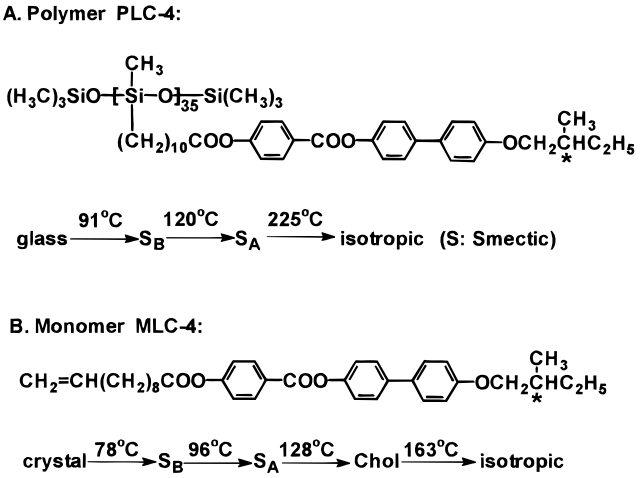

Figure 1. Chemical structures of investigated compounds.

Pure and mixed monolayers were characterized by surface pressure−area isotherm and hysteresis curves to exploit the phase transition and the possible molecular arrangement. Multilayers' structures were analyzed by small angle X-ray diffraction and UV−visible absorption.

Experimental Section

The synthesis and characterization of the materials under investigation are discussed in more detail elsewhere.[26] The polymer was synthesized by hydrosilication addition of Si−H to a carbon−carbon double bond using a Pt complex as the catalyst to obtain a comblike liquid crystalline polymer. The monomer was purified by recrystallization from ethanol, followed by silica gel chromatography. The polymer was purified by several reprecipitations from chloroform solution into methanol. Arachidic acid (AA) in HPLC grade was obtained from Sigma Chemical Co. and used as received. The

* To whom correspondence should be addressed.

[⊗] Abstract published in *Advance ACS Abstracts,* July 1, 1996.

S0024-9297(95)01803-1 CCC: $12.00

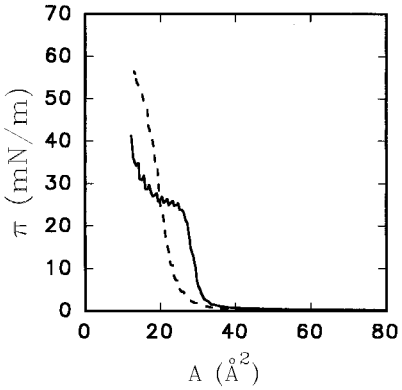

Figure 2. Surface pressure−area isotherms for pure MLC-4 (solid line) and PLC-4 (dashed line) monolayers.

chloroform used as solvent was reagent grade and was redistilled before use to remove any nonvolatile impurities.

The experiments for monolayer spreading and deposition of the LB film were performed on a commercially available Langmuir trough NIMA 2000 (NIMA Technologies) with computerized control and two working modes (single or two barrier compression). A Wilhelmy balance was used as a surface pressure sensor. All measurements were carried out at room temperature (20 ± 1 °C). Surface areas are reported in square angstroms per molecule for the monomer and square angstroms per mesogenic repeating unit for the polymer.

Monolayers were obtained by spreading chloroform solutions of the compounds, with concentrations between 0.2 and 0.6 mg/mL. The water used for the subphase was prepared from redistilled water (pH = 6.2). After spreading, 10 min was allowed for solvent evaporation, and then the film was compressed at a barrier speed ranging from 2 to 10 Å²/(repeat unit min) (typically ≅ 4 Å²/(repeat unit min)). In hysteresis experiments, the barrier movement was immediately reversed after the pressure reached the desired value.

When measuring isotherms for pure LC compounds, it was important to use symmetric compression barriers with the Wilhelmy plate in the middle of the trough facing parallel to the moving barriers for reproducible results. Because the polymer monolayers were viscous and rigid at high applied surface pressures, erroneous data were easily induced due to the deflection of the Wilhelmy plate if one barrier was used. All isotherms and hysteresis curves were run a minimum of three times with reproducibility errors of less than ±1 Å².

LB films were built up on glass or quartz plates by the vertical dipping method. The typical dipping rate was 10 mm/min. The substrates were hydrophobized with trimethylchlorosilane (Merck, Germany) after being rigorously cleaned with chromic acid.

Small angle X-ray diffraction patterns were obtained using a D/MAX-γB X-ray diffractometer with Cu Kα radiation (λ = 0.154 nm). The multilayers deposited on microscope slides were examined.

A Schimadzu recording spectrometer (model UV-3000) was used to take UV−visible absorption spectra. The bulk spectrum was obtained from an *n*-hexane solution of about 0.05 mg/mL (diluted from stock) of the PLC-4 in a fused silica cell with a path length of 1 cm. Hydrophobized fused silica plates were used for measurements of absorption of LB films.

Results and Discussion

Although the materials used in our investigation were not specially designed as amphiphiles, all can be spread from a chloroform solution onto the water surface to form monomolecular films.

Isotherms for the Monomer MLC-4. Figure 2 shows the surface pressure (π)−area (A) isotherms of the MLC-4 and PLC-4. The curve of the monomer exhibits only a liquid-condensed phase upon compression. The collapse pressure (π_c) of MLC-4 is about 23 mN/m, the lowest of the investigated compounds and blends, indicating its lower film stability. After the collapse point the surface pressure increases with little fluctuation, corresponding to the formation of a solidlike phase, that is, aggregates or crystallites. Such phase assignments have also been confirmed by in situ Brewster angle microscopy (BAM) observations.[35] Above π_c the monolayer showed a larger incompressibility and concave lines with further compression. When the monolayer was expanded at this moment, only rigid fragments could be observed, which were not spread again.

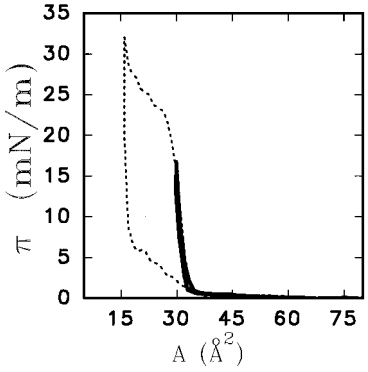

Figure 3. Hysteresis curves in the first run of the compression−expansion cycle for the MLC-4 monolayer with reversed pressure at 15 mN/m (solid line) and 30 mN/m (dashed line), respectively.

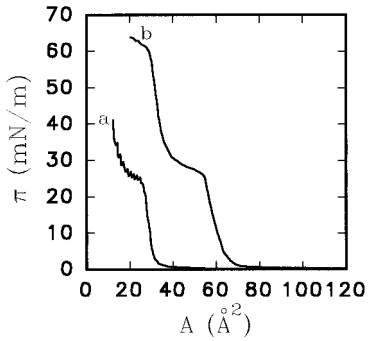

Figure 4. Surface pressure−area isotherms for the pure MLC-4 monolayer and AA/MLC-4 mixed monolayer: (a) pure MLC-4; (b) AA:MLC-4 = 1:1.

Results of hysteresis experiments (shown in Figure 3) reveal that a large hysteresis appears when the reverse pressure is larger than the π_c and the second compression after the pressure release results in the reduction of the average surface area per molecule (A_0) and only a steep increase of π. We consider that it may be due to the formation of aggregates by MLC-4 molecules in the monolayer at higher pressures which do not spread after the pressure release. The aggregation leads to a higher packing density and hence a dramatic increase of π. Results from the third compression also support the above opinion because the curve basically coincides with the second one, which indicates that the molecular packing is too dense to be compressed. The average surface area per molecule A_0 obtained by extrapolation from the linear region (corresponding to a condensed film) to zero pressure is 31.4 Å², larger than the calculated cross-sectional area of the planar biphenyl (22.9 Å²),[27] which implies the chains twist and tilt to some extent in the monolayer.

Figure 4 exhibits isotherms of the monomer and its blends with arachidic acid at a molar ratio of 1. Because the materials in our research are not typical amphi-

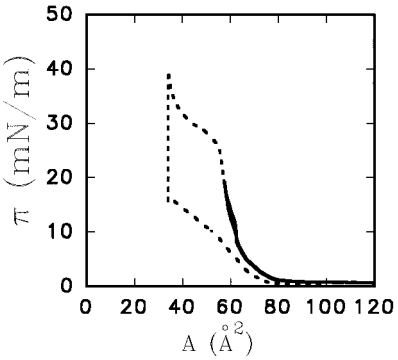

Figure 5. Hysteresis curves for AA/MLC-4 mixed monolayers (molar ratio 1:1) with reversed pressure at 20 mN/m (solid line) and 40 mN/m (dashed line), respectively.

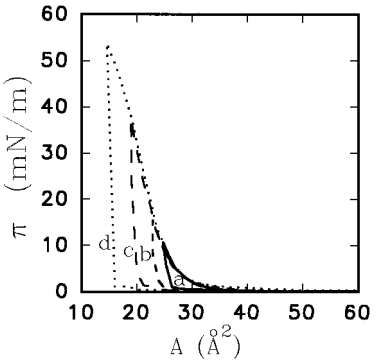

Figure 6. Hysteresis curves for the PLC-4 monolayer with different reversed pressures: (a) 10 mN/m; (b) 20 mN/m; (c) 40 mN/m; (d) 55 mN/m.

philes and usually form rigid and viscous monolayers which are difficult to transfer for LB film preparation, we incorporate MLC-4 and PLC-4 molecules into matrices of AA to fabricate a stable and easily transferable film of these compounds. AA can not only plasticize the side chains, which are quite rigid due to the strong interaction between the mesogenic cores, but also add a more defined hydrophobic region to the film in order to "anchor" the film out of the water phase. To do so can promote the orientation of the mesogenic side chains in the packing lattice as well. From Figure 4, it is clear that the collapse pressure increases notably to about 60 mN/m for the AA/MLC-4 blend and an inflection region at about 26 mN/m appeared on the isotherm, which is speculated from the following hysteresis experiments to be an irreversible phase transition from the liquid-condensed to a solidlike phase. The A_0 values extrapolated before and after the inflection are 65.5 and 44 Å^2, respectively. The former is larger than that calculated by considering the cross-sectional areas of AA (20.5 Å^2) and planar biphenyl (22.9 Å^2). But the latter is very close to the sum of these two components. From these results we get a picture of the mixed monolayer: MLC-4 molecules are distributed uniformly with AA. In this case, MLC-4 chains cannot get close enough to each other, as in their pure state. AA molecules prevent MLC-4 chains from aggregating or tangling up effectively. Considering the poor amphiphilicity of MLC-4 molecules, we should still assume the tilted orientation of MLC-4 chains. All these factors result in a larger area per molecule before the monolayer is compressed to the inflection region. If MLC-4 and AA molecules are separated into different phases, the MLC-4 molecules will be expected to twist, collapse, or aggregate to crystallites as π is raised, as observed for pure MLC-4. Such effects, however, will result in a smaller value of the apparent surface area. In the inflection region, we think, due to support by AA molecules the MLC-4 molecules become dense packed with chains nearly perpendicular to the subphase surface.

Figure 5 shows hysteresis curves for reverse pressure above and below the inflection region when the mole fraction of MLC-4 is 0.5. It can be observed that there is only a little hysteresis in the compression−expansion cycle before the inflection pressure, showing reversible behavior. Nevertheless, a large hysteresis of the irreversible compression−expansion cycle occurs if the reverse pressure is higher than the inflection point. So we conclude that a certain process occurs in the mixed film at the inflection region and causes molecules to arrange in a denser pattern. Comparing isotherms of pure and mixed films of MLC, we think this region may correspond to a phase transition from a liquid-condensed film to a solidlike film.

Isotherms of Polymer PLC-4. The isotherm of polymer PLC-4 (Figure 2, dashed line) shows dissimilarities with the monomer isotherm. On one hand, it does not show any phase transition in the stable monolayer region but exhibits a more condensed compressibility. On the other hand, the collapse pressure is significantly increased (>50 mN/m) and the isotherm shows some dependence on compression speed. In general, the limiting area A_0 was observed to decrease with increasing compression rate. This is a common behavior observed with polymers and can be attributed to relaxation at the surface with slower compression speeds.[28] Thus, not unexpectedly, it appears that the PLC-4 monolayer is more viscous than the monomer monolayer.

It should be noted that the PLC-4 monolayer is highly rigid and viscous. The reproducible isotherm can only be obtained with the Wilhelmy method if the Wilhelmy plate is positioned in the center of the trough and two barriers are compressed symmetrically from both sides. Otherwise, the plate may be squeezed out of its normal position easily by the rigid film. Furthermore, there are large gradients in the actual surface pressure along the length of the monolayer.[29] These effects all produce large errors in pressure measurement.

Extrapolation of the linear high-pressure region to zero pressure results in the compression speed dependent area per mesogenic repeat unit of 23.8 Å,^{2} approximately corresponding to the cross-sectional area of the mesogen unit oriented perpendicular to the air/water interface. Compared to the monomer case, this indicates that the siloxane backbone in the polymer is far more crucial in the monolayer packing of the mesogenic side chains. The extension of the siloxane backbone and its probable interaction with the water surface can reduce the possible twist, tilt, and other irregular arrangements that usually occur for monomer chains. These actions also prevent any extensive interaction between the side chain mesogenic groups and lead to closer packing. This might explain the high π_c that is observed for PLC-4.

Results of hysteresis experiments of the PLC-4 monolayer are very similar to those of the monomer at high π. Even at small π, large hysteresis cycles can still be seen (Figure 6), implying large film rigidity and viscosity. Following compressions only a steep rise in pressure is seen, characteristic of solidlike packing. This behavior has been attributed before to rearrangement in the monolayer.[30] Probably, when the monolayer is initially spread at the air/water interface, the polymer

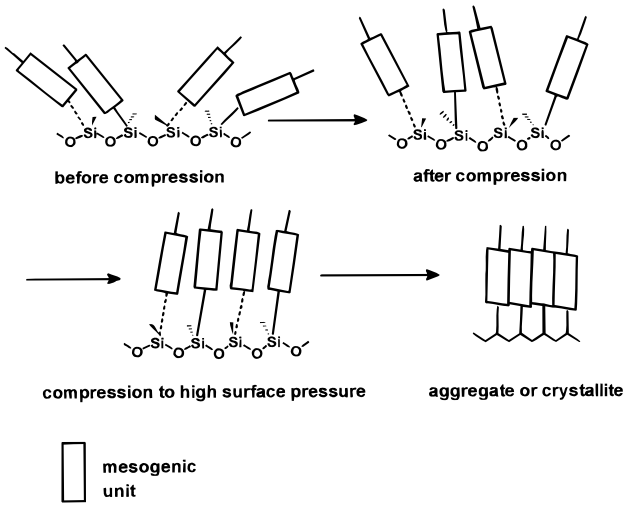

Figure 7. Arrangement of side chains during compression.

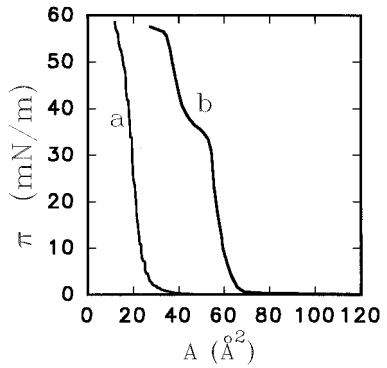

Figure 8. Surface pressure−area isotherms for AA/PLC-4 mixed monolayers: (a) pure PLC-4; (b) AA:PLC-4 = 1:1.

molecules are uniformly distributed on the surface with their backbones at the interface and the side chains tilted toward the air. As the pressure increases during the first compression, the side chains tilt further away from the water and start packing tightly. Since the side chains are longer, they may aggregate to form crystallites and, after the pressure is released, they do not respread to the same state. Instead, they could remain on the water surface as islands of crystallites. This process is schematically shown in Figure 7.

As done in monomer monolayer studies, the PLC-4 molecules were mixed with AA to reduce the rigidity and viscosity of the film. Another important reason for mixing is to improve the deposition properties of PLC-4 because polymers with longer side chains (C_{14} and above) form only rigid solid monolayers which tend to crystallize after the initial compression and are difficult to transfer.[31] The miscibilty of these two components can be analyzed from the surface pressure−area isotherms. A complete additive behavior of properties of the compounds can demonstrate either an ideal behavior or complete immiscibility. Figure 8 compares isotherms for PLC-4 and its blend with AA at a molar ratio of 1. The curve of the blend exhibits a distinct inflection in the pressure−area response compared to that of the pure polymer. Values of the apparent area taken by mesogenic repeat unit (A_0), extrapolated from the linear high-pressure regions before and after the inflection point, are 60 and 52 Å^2, respectively. Both of them are larger than the sum of the cross-sectional area for each component calculated according to the composition, indicating the side chains do not reach the closest packing in AA matrices. Smaller values of A_0 after the

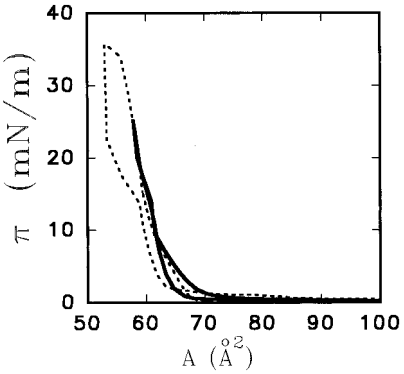

Figure 9. Hysteresis curves for the AA/PLC-4 = 1:1 mixed monolayer with reversed pressure at 25 mN/m (solid line) and 35 mN/m (dashed line), respectively.

inflection, however, can give us an enlightenment that the monolayer undergoes a phase transition at the inflection. The deviation from additive behavior suggests molecular miscibility of AA and PLC-4.[28] At the air/water interface the hydrophilic parts of AA (COOH) and PLC-4 (siloxane backbone) are oriented toward the water surface and their hydrophobic parts (alkyl chains and mesogenic side chains) are oriented away from the water surface. It is conceivable that this orientation brings the chemically similar parts into close contact and facilitates intermolecular interactions. So molecules can be compatible at the air/water interface. BAM observations also show miscibility of AA and PLC-4 because no phase-separation images could be observed.

In order to better understand the nature of this phase transition, we measured hysteresis curves with the compression direction reversed before and after the inflection, respectively (see Figure 9), and obtained results very similar to those of mixed monolayers of monomer. It is observed that little hysteresis and good reproducibility belong to the compression−expansion cycle below the inflection but relatively excessive hysteresis and irreversibility appear for compression to pressures higher than the inflection point. From this we suggest that PLC-4 exists as an ordered fluid phase in the mixed monolayer below the transition region. The siloxane backbone in the matrices of AA can extend to some extent. Therefore the mesogens cannot get close enough to each other to be dense packed normal to the plane of the monolayer and must assume a tilted conformation. Above the inflection pressure, the mixed film is a highly incompressible solid film. At this time we must assume that the mesogenic side chains are more perpendicular to the water surface and get close together from the two sides of the main chain to ensure denser packing of the mesogens (as seen in Figure 7).

The phase-transition phenomena occurring in and around the inflection region were also inspected by AFM and TEM observations.[35] All results obtained clearly indicate that the mixed monolayer undergoes a phase-transition from an amorphous liquid condensed state to a crystalline stacked pattern.

Deposition of LB Films. In this section, results from the polymer studies are discussed. To prepare LB films of blends for PLC-4 and AA, we examined the surface area (A)−time (t) isobars at pressures below or above the inflection region. The results show that the mixed films are stable enough to be deposited.

Combining data from π−A and A−t experiments, we carried out most monolayer transfers at 20 mN/m. To compare the effects of AA's proportion and surface

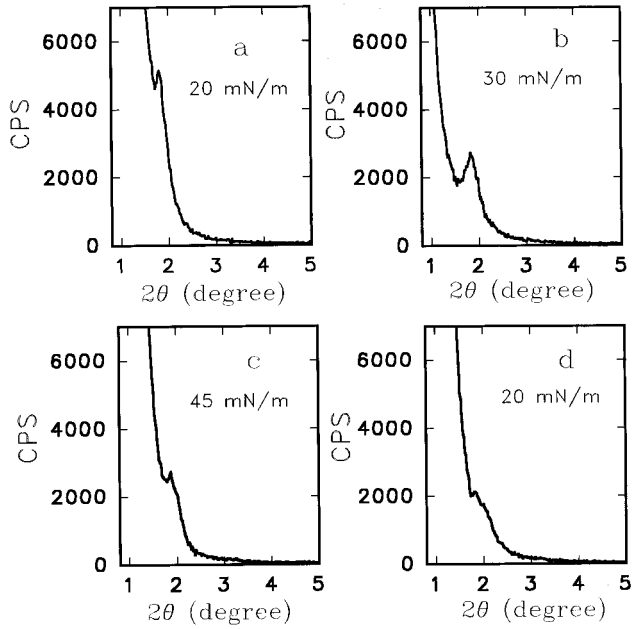

Figure 10. X-ray diffraction patterns from mixed LB films: AA:PLC-4 = 1:1 for (a)−(c) and 1:3 for (d) (20 layers).

Table 1. Layer Spacings for AA/PLC-4 Mixed LB Films

deposition pressure (mN/m)	AA:PLC-4 = 1:1			AA:PLC-4 = 1:3
	20	30	45	20
layer spacing (Å)	48.0	48.0	47.0	46.5

pressure on the molecular packing, LB deposition was also done for the blend with AA:PLC-4 = 1:3 at 20 mN/m and blends with AA:PLC-4 = 1:1 at 30 and 45 mN/m. All mixed films were transferred to the hydrophobic substrates at a rate of 10 mm/min. When hydrophilic substrates were used at the same pressure, the layer deposited on the upstroke would quantitatively "peel off" the substrate on the next downstroke. These observations may be related to the short delay time (5−6 min) after upward dipping, not long enough to dry the film which is often described as necessary for a successful transfer of a large number of layers.[32] When layers are deposited at 20 mN/m, we get Y-type films with a transfer ratio between 0.8 and 0.9.

X-ray Diffraction. Parts a−d of Figure 10 show X-ray diffraction patterns in the small angle region for LB films (20 layers) with different mixing ratios and deposition pressures. Several diffraction peaks are visible, exhibiting some layer orders in the direction of the substrate normal. The averaged layer spacings calculated from the first peak according to the Bragg equation are listed in Table 1. Corresponding to molar ratios (AA/PLC-4) of 1:1 and 1:3, we get layer spacings of 48.0 and 46.5 Å, respectively. The smaller spacing for the latter is speculated to be the result of a lack of AA's support. It should be noted that, however, the absence or haziness of the second- or third-order peaks in the diffractograms indicates the layer orders are not so well-defined as LB films formed by typical amphiphiles. Though the inhomogeneity of the mixed LB films had also been reflected by the low transfer ratios in upstrokes which were often between 0.7 and 0.8, the nearly linear relationship of UV absorption peak intensities to layer numbers still suggested the existence of layered film structures.

Comparing the chain length of AA (26.9 Å) and the calculated length of the side chain group including the siloxane backbone (approximately 40 Å)[33] with the obtained layer spacings, we speculate that the Y-type mixed LB film has a tilted layer structure. The polarized IR spectra carried out recently for AA/PLC-4 mixed LB films[35] give strong support to this structural assertion, which show that the side chains are inclined at about 57° to the film normal.

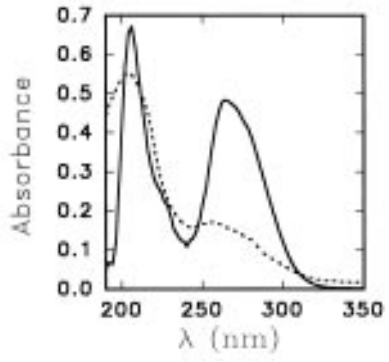

Figure 11. UV−vis spectra for PLC-4 in *n*-hexane solution (solid line) and the 32-layer AA:PLC-4 = 1:1 mixed LB film deposited at 20 mN/m (dashed line).

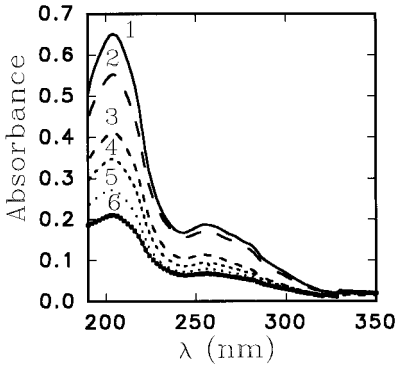

Figure 12. UV−vis spectra for AA:PLC-4 =1:1 mixed LB films deposited at 20 mN/m with different layers: (1) 40; (2) 32; (3) 24; (4) 20; (5) 16; (6) 12.

It should be noted that the irregular smaller spacing for the film deposited at 45 mN/m reflects a somewhat different film structure and can be considered as a deformed conformation of side chains due to the formation of aggregates or crystallites, which has been confirmed by the crystalline hexagonal pattern in electron diffraction measurements.

UV−Visible Spectra. Figure 11 shows the nonpolarized UV−visible spectra obtained from *n*-hexane solutions of the polymer and the LB layers. For PLC-4 solution there exist two strong absorption peaks at 264 and 206 nm, corresponding to the $\pi \rightarrow \pi^*$ transition of the aromatic ring and E band of the benzene ring, respectively.

A distinct hypsochromic shift is observed for the mixed LB multilayer compared with the solution. The band is shifted from 264 nm in the solution spectra to 255 nm for the LB films. The shift is indicative of a linear aggregation of mesogenic units with their transition moments parallel to each other, arranged perpendicular or slightly tilted to the stacking direction (H aggregation).[34] The difference in the relative intensities of the absorption bands is thought to be primarily due to the inherent orientation properties of the LB films.

Figure 12 shows the absorption spectra for LB films with different layer numbers. It can be observed that the positions of absorption peaks do not move and there is a nearly linear relationship of peak intensities to layer numbers. This, with the X-ray data, indicates homo-

geneous transfer, and no aggregation occurs between molecules in different layers.

Conclusions

From the above data and discussions, it is concluded that the materials under investigation can form monolayers at the air/water interface. The polymer formed much more stable films than the monomer. Matrices of AA can improve the packing of side chains and enhance the film stability. At higher surface pressures, molecules aggregate or crystallize to form islands with solidlike stacking. The mixed films can be transferred onto hydrophobic substrates. X-ray diffraction and UV−visible spectra confirm that the LB films have a tilted layered structure similar to that in bulk smectic phases and there exists indeed axial order in the mixed multilayers. The LB technique is thus an efficient method of systematically manipulating the layer-to-layer stacking order of the liquid crystalline polymer. Spectroscopic investigations by IR and UV−vis with polarized light and morphology observation by BAM are still in progress, which may give more insight into the properties of the ferroelectric polymers at the interface.

Acknowledgment. This work was supported by the National Natural Science Foundation of China and State Major Basic Research Project. The authors thank the Key Laboratory for Colloid and Interface Chemistry of State Education Commission for supporting the BAM experiments.

References and Notes

(1) Eich, M.; Wendroff, J. *J. Opt. Soc. Am.* **1990**, *B7*, 1428.
(2) Assanto, G.; Neher, D.; Stegeman, G. I.; Torruellas, W. E.; Margues, M. B.; Horsthuis, W. H. G.; Mohlmann, G. R. *Mol. Cryst. Liq. Cryst.* **1992**, *222*, 33.
(3) Ozaki, M.; Sakuta, M.; Yoshino, K.; Helgee, B.; Svensson, M.; Skarp, K. *Appl. Phys. B* **1994**, *59*, 601.
(4) Ozaki, M.; Utsumi, M.; Yoshino, K.; Skarp, K. *Jpn. J. Appl. Phys.* **1993**, *32*, L852.
(5) Shashidhar, R.; Naciri, J.; Pfeiffer, S.; Fare, T. L. U.S. Patent US 5,293,261 (CL. 359-87; G02F1/13), 08 Mar 1994.
(6) Nakamura, T.; Ueno, T.; Tani, C. *Mol. Cryst. Liq. Cryst.* **1989**, *169*, 167.
(7) Sasaki, A. *Mol. Cryst. Liq. Cryst.* **1986**, *139*, 103.
(8) Ulman, A. *An Introduction to Ultrathin Organic Films*; Academic Press: New York, 1991.
(9) Roberts, G. G., Ed. *Langmuir−Blodgett Films*; Plenum: New York, 1990.
(10) Tieke, B. *Adv. Mater.* **1990**, *2*, 222.
(11) Sakuhara, T.; Nakahara, H.; Fukuda, K. *Thin Solid Films* **1989**, *159*, 345.
(12) Adams, J.; Rettig, W.; Duran, R. S.; Naciri, J.; Shashidhar, R. *J. Phys. Chem.* **1993**, *97*, 2021.
(13) Adams, J.; Buske, A.; Duran, R. S. *Macromolecules* **1993**, *26*, 2871.
(14) Thibodeaux, A. F.; Rädler,U.; Shashidhar, R.; Duran, R. S. *Macromolecules* **1994**, *27*, 784.
(15) Fadel, H.; Percec, V.; Zheng, Q.; Advincula, R. C.; Duran, R. S. *Macromolecules* **1993**, *26*, 1650.
(16) Rettig, W.; Naciri, J.; Shashidhar, R.; Duran, R. S. *Macromolecules* **1991**, *24*, 6539.
(17) Rettig, W.; Naciri, J.; Shashidhar, R.; Duran, R. S. *Thin Solid Films* **1992**, *210/211*, 114.
(18) Ou, S. H.; Percec, V.; Mann, J. A.; Lando, J. B.; Zhou, L.; Singer, K. D. *Macromolecules* **1993**, *26*, 7263.
(19) Carpenter, M. M.; Prasad, P. N.; Griffin, A. C. *Thin Solid Films* **1988**, *161*, 315.
(20) Vandevyver, M.; Keller, P.; Rouillay, M.; Bourgoin, J-P.; Barraud, A. *J. Phys. D: Appl. Phys.* **1993**, *26*, 686.
(21) Ali-Adib, Z.; Tredgold, R. H.; Hodge, P.; Davis, F. *Langmuir* **1991**, *7*, 363.
(22) Menzel, H.; Weichart, B.; Schmidt, A.; Paul, S.; Knoll, W.; Stumpe. J.; Fischer, T. *Langmuir* **1994**, *10*, 1926.
(23) Menzel, H.; Weichart, B.; Hallensleben, M. L. *Thin Solid Films* **1993**, *223*, 181.
(24) Chen, X.; Xue, Q. B.; Yang, K. Z.; Zhang, Q. Z. *Langmuir* **1995**, *11*, 4082.
(25) Pfeiffer, S.; Shashidhar, R.; Fare, T. L.; Naciri, J.; Adams, J.; Duran, R. S. *Appl. Phys. Lett.* **1993**, *63*, 1285.
(26) Zhang, Q. Z.; Xue, Q. B. *Proceedings of the International Conference on Liquid Crystalline Polymers (IUPAC)*; Beijing: China, 1994; p108.
(27) Hargreaves, A.; Rizvi, S. H. *Acta Crystallogr.* **1962**, *15*, 365.
(28) Gains, G. L., Jr. *Insoluble Monolayer at Liquid Gas Interface*; Wiley: New York, 1966.
(29) Peng, J. B.; Barnes, G. T. *Langmuir* **1990**, *6*, 578.
(30) Gains, G. L., Jr. *Langmuir* **1991**, *7*, 834.
(31) Rodriguez-Parada, J. M.; Kaku, M.; Sogah, D. Y. *Macromolecules* **1994**, *27*, 1571.
(32) Erdelen, C.; Laschewsky, A.; Ringsdorf, H.; Schneider, J.; Schuster, A. *Thin Solid Films* **1990**, *180*, 153.
(33) Weast, R. C., Ed. *CRC Handbook of Chemistry and Physics*; CRC Press: Boca Raton, FL, 1984; pp f-166.
(34) Umemua, J.; Hishiro, Y.; Kawai, T.; Takanaka, T.; Gotoh, Y.; Fujihira, M. *Thin Solid Films* **1989**, *178*, 281.
(35) Chen, X.; Xue, Q. B.; Yang, K. Z.; Zhang, Q. Z. Manuscript in preparation.

MA951803N